Eur. Phys. J. D (2015) 69: 43
DOI: 10.1140/epjd/e2014-50525-4

THE EUROPEAN PHYSICAL JOURNAL D

Regular Article

Investigation of quantum coherence effects in a multilevel atom induced by three laser fields

Saswati Dey, Nilanjan Aich, Chanchal Chaudhuri, and Biswajit Ray[a]

Department of Physics, University of Calcutta, 92 A.P.C. Road, 700009 Kolkata, India

Received 17 July 2014 / Received in final form 29 September 2014
Published online 12 February 2015 – © EDP Sciences, Società Italiana di Fisica, Springer-Verlag 2015

Abstract. In this work, we report a detail theoretical study to understand the quantum coherence processes induced by three laser fields in a multilevel atom. In one of the coupling scheme using three laser fields we have theoretically simulated the EIA and EIT resonances simultaneously in a single probe transmission profile. It has been shown that these two coherent resonances of opposite kinds can be tuned at any position of the probe profile and they cancel out when they are completely merged together. We have also theoretically calculated the dual-EIT as well as a single EIT resonance with improved contrast in an N-type scheme. It has been shown that the contrast of the V-type EIT is greatly enhanced in the N-type system when it is tuned to the position of Λ-type EIT. We have examined the atomic density effect on the enhanced N-type EIT resonance and it has been shown that the nature of variation of the line shape of this pronounced EIT resonance strongly depends on the variations of the individual Λ- and V-type EIT with atomic density. Theoretically simulated spectra have been compared with the experimental observations in rubidium vapour with its natural abundances. For the experimental comparison of the observed resonances under different atom-laser coupling schemes, we have used the D_2 transition ($5S_{1/2}$–$5P_{3/2}$) of ^{85}Rb isotope. A good agreement is found between the simulated results and the experimental spectra.

1 Introduction

Quantum interference between atomic states caused by atom-laser interaction modifies the optical properties of an atomic medium producing coherent resonances like coherent population trapping (CPT) [1], electromagnetically induced transparency (EIT) [2,3] and electromagnetically induced absorption (EIA) [4,5]. The formation of EIT in Λ-type system is based on the idea of CPT [6]. In the Λ-type configuration one can get a good contrast EIT resonance as the coherence dephasing rate comes to play between the ground hyperfine levels. Since the CPT effect cannot be established in a V-type system due to the spontaneous decay from the excited hyperfine levels, this particular configuration produces the poorest EIT. In the V-type system EIT can be obtained only due to the destructive quantum interference between the transition pathways of the pump-probe laser fields. On the contrary, electromagnetically induced absorption i.e. EIA resonance is of completely opposite nature in comparison to EIT resonance. Constructive quantum interference between the excitation pathways of the pump-probe lasers leads to the EIA resonance. Since the EIA resonance shows anomalous dispersion it plays a major role in superluminal propagation of light [7].

Since the discovery of EIT it had been well studied both theoretically and experimentally by many authors in three basic level schemes Λ, V and Ξ [8–12] by using two coherent fields namely pump and probe laser fields. In recent times the studies of the quantum interference effects in different kinds of level configurations using more than two coherent fields are drawing more attention than the simple basic level schemes [13–17]. When a multilevel atomic system interacts with several radiation fields interesting coherent features can be obtained due to the contribution from the hyperfine levels as well as the degenerate Zeeman levels corresponding to these hyperfine levels. The investigation of the coherent resonances arising from the quantum interference effects in presence of three laser fields are very important for their applications in four-wave and six-wave mixing processes [18], producing the ultraslow light for optical information processing [19], optical switching [20] and multi channel communication [21].

In this paper, we have theoretically investigated the coherent resonances produced by two different coupling schemes in the ^{85}Rb-D_2 transition by using three laser beams namely pump, control and probe lasers. In one of such configuration we have obtained simultaneously the EIT and EIA resonances in a common probe transmission profile. Both of the EIT and EIA resonances strongly depend on the laser field polarization as the line shape of the resonances changes dramatically depending upon the polarization combination of the laser fields [22,23]. To obtain the good contrast of EIT resonance we have chosen here all three laser fields as linearly polarized and

[a] e-mail: brphys@gmail.com

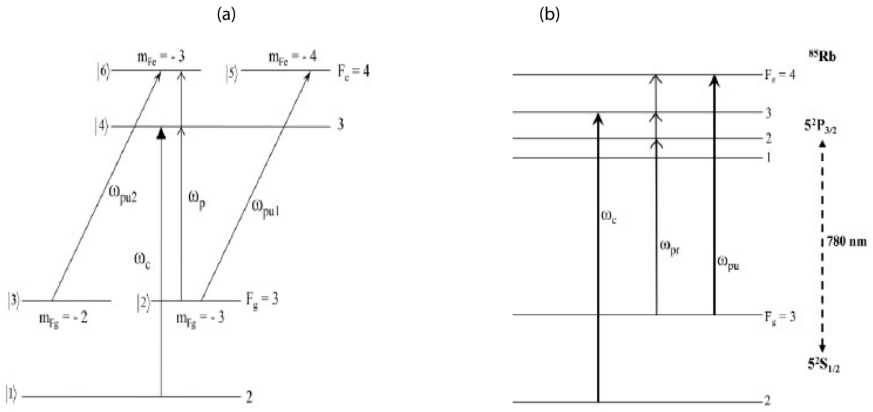

Fig. 1. (a) Energy level diagram for the theoretical formulation to get the EIA and EIT resonances simultaneously; (b) represents the experimental energy level diagram for a multilevel system coupled by three laser fields in ^{85}Rb-D_2 transition.

the polarization of the control and pump lasers are orthogonal to the probe laser field. In order to theoretically model the EIA phenomenon by a degenerate N-type system, we have considered linear orthogonal polarization of the probe and pump laser fields. Such polarization combination leads to more number of coherently coupled N-type systems which contribute together in the formation of the EIA resonance [23]. Here we have theoretically presented the effect of individual tuning of the pump and the control lasers over the probe Doppler profile and in both cases we have shown that the EIT and EIA resonances can be tuned very close to each other. Since these two coherent resonances originate from two opposite effects, therefore by proper tuning of the pump or control laser fields, both of the EIT and EIA resonances can also be made to disappear completely in the probe transmission profile. EIT and EIA affect the multi-wave mixing process in atomic media and the observation of the wave mixing process at the probe frequency position where the EIT and EIA are very close to each other or completely merged may be useful. We have performed an experiment with three lasers to observe the EIA and EIT resonances simultaneously in a single probe Doppler profile in the D_2 line of ^{85}Rb isotope and observed that both of the coherent resonances disappear completely whenever the EIT window gets superimposed with the EIA resonance. In another system forming an N-type configuration interacting with three lasers, we have shown the dual-EIT in a single probe transmission profile in the theoretical simulation and the two distinct transparency peaks are obtained due to the detuned frequency position of the control laser with respect to the pump laser. Study of dual-EIT is also useful in four wave mixing process under EIT condition [18]. With proper tuning of the pump and control laser fields the two EIT peaks are merged and a single and enhanced EIT peak is obtained. Theoretical results corresponding to this configuration are also established by the experimental observations in presence of three laser beams. The dual-EIT resonances with different detuned frequency positions of the control laser over the probe Doppler profile have been studied. The line shapes of the EIT resonances get significantly modified with the change in the atomic number density. In our previous work [12], we discussed the atom density effect on EIT resonances in the individual Λ- and V-type systems. In this work, we have simulated this density effect on the merged EIT resonance in the N-type system incorporating relevant parameters. The N-EIT peak, which is a superposition of Λ and V-EIT, shows an interesting nature of variation for the increment in the atomic number density. To experimentally investigate the density effect on the single N-EIT peak, we have increased the temperature of the vapour cell that results in the increment of the density of the atoms in the cell. Simulated results are found to be consistent with the observations.

2 Theoretical calculation and experimental comparison for simultaneous EIT and EIA resonances

In this section, we have first made a theoretical simulation of the simultaneous EIT and EIA resonances in a single probe transmission profile in presence of a pump and control laser fields. Let us consider that F_g and F_e are respectively the ground and excited hyperfine levels of the multilevel atom. When the probe and the pump laser fields induce the transition $F_g \rightarrow F_e$, then the coherence between the degenerate excited and ground magnetic sublevels corresponding to these hyperfine levels produces the enhanced absorption dip i.e. EIA resonance in the probe transmission. The EIA resonance appears for the transition $F_g \rightarrow F_e$ when the following conditions are satisfied: (i) $F_g > 0$, (ii) $F_e = F_g + 1$ and (iii) $F_g \rightarrow F_e$ transition must be closed. If an additional laser, say, control laser is applied from the other ground hyperfine level $(F_g - 1)$ to the possible excited hyperfine level in the same atomic system, then the control and probe lasers produce the EIT resonance forming a Λ-type configuration. Therefore, in presence of three laser beams namely pump, control and probe, it is possible to produce the coherent resonances of opposite kinds in a single atomic system. The theoretical energy level diagram producing both EIA and EIT resonances is shown in Figure 1a. The control laser of frequency ω_c, applied from the ground level $|1\rangle$ to the

excited level $|4\rangle$ forms the Λ-type system with the probe laser (ω_p) scanning from the other ground level $|2\rangle$ to the excited level $|4\rangle$. This Λ-type system leads to an EIT resonance due to coherence created between the ground levels. The occurrence of the EIA resonance is explained as the transfer of coherence from degenerate excited levels to the degenerate ground levels via spontaneous emission [4]. So we have constructed a degenerate N-type system between the levels $|2\rangle$, $|3\rangle$, $|5\rangle$ and $|6\rangle$ to produce the EIA resonance theoretically. The N-type system between the degenerate levels is formed when the pump laser of frequency ω_{pu} induces the transitions from the ground degenerate magnetic sublevels $|2\rangle$ and $|3\rangle$ to the excited degenerate magnetic sublevels $|5\rangle$ and $|6\rangle$, respectively, with the probe laser connecting the ground level $|2\rangle$ to the excited level $|6\rangle$. Such degenerate Zeeman levels can be obtained in the hyperfine structure of the alkali atoms. The optical Bloch equations for the entire system are derived from the Liouville's equation,

$$i\hbar\frac{\partial\rho}{\partial t} = [H,\rho] + \xi\rho \tag{1}$$

where 'H' ($=H_0 + H_p$) represents the total Hamiltonian of the system including the unperturbed (H_0) as well as the perturbation term (H_p). ξ is the relaxation operator and ρ is the density matrix operator. H_0 and H_p are expressed as,

$$H_0 = \sum_{i=1}^{6} \hbar\omega_i \,|i\rangle\langle i| \tag{2}$$

$$H_p = \frac{\hbar}{2}\Big[\Omega_p\left(|4\rangle\langle 2| + |6\rangle\langle 2|\right)e^{-i\omega_p t} + \Omega_{pu1}\,|5\rangle\langle 2|\,e^{-i\omega_{pu1}t} + \Omega_{pu2}\,|6\rangle\langle 3|\,e^{-i\omega_{pu2}t} + \Omega_c\,|4\rangle\langle 1|\,e^{-i\omega_c t} + c.c\Big]. \tag{3}$$

The optical Bloch equations that are derived from equation (1) using rotating wave approximation (RWA) are given in Appendix A. The Bloch equations include all possible system relaxations, dephasing and the term corresponding to the transfer of coherence for the EIA system. In this model the hyperfine and Zeeman optical pumping effect corresponding to the multilevel atomic system is taken into account by the relaxation of population via the spontaneous decay from the excited to all allowed ground states. The population redistribution between the ground levels due to the optical pumping effect is expressed as $A_{ji}\Gamma_j\rho_{jj}$ (see Appendices), where A_{ji} includes the branching ratio and the laser intensity. The optical pumping time is inversely proportional to the laser intensity and also includes the branching ratio of the relaxation processes [24]. It was suggested by Smith and Hughes [25] that the time needed for optical pumping is very short, typically of the order of tens of nanosecond for the on-resonant frequency of the pump laser, but in the year 2006, Maguire et al. [26] had shown that the pumping process is slow enough, typically of the order of 50 lifetimes (1.5 μs for ^{85}Rb). Optical pumping is a transient phenomenon and many authors have utilized the method of the interaction time average of the density matrix to produce more accurate results [27–29]. In this present work regarding the multilevel atomic structure, we have numerically solved the density matrix equations under steady state condition and the simulated results are found to agree well with the experimental findings. In our case considering a typical cm size cell and a laser beam diameter of 2 mm, the atomic transit time (τ_f) through the laser beam is turned out to be 8 μs. The shape of the coherent resonances in an atomic system strongly depends on the ground state decoherence which may be caused by several mechanisms like transit time relaxation, atom-atom or atom-wall collisions in the vapour cell, etc. We have taken into account all of the possible ground state decays in our theoretical calculation. The coherence dephasing rate (γ_{j1}) can be due to different kinds of collisions in the vapour cell like atom-atom and atom-wall collisions, etc. Γ_{ii}^{N} accounts for the incoherent mixing of the ground state population due to thermal excitation as well as the population exchange between the ground states via transit relaxation [30]. In order to obtain the Doppler free probe transmission, the set of optical Bloch equations are solved numerically for atoms with a particular velocity 'v' to obtain the non-diagonal density matrix elements ρ_{i2} ($i = 4, 6$). The imaginary part of the sum of these matrix elements would yield the Lorentzian profile of the probe transmission line shape $\chi(\omega_P, v)$. The Doppler-broadened probe transmission spectrum can be obtained taking into account the Maxwell-Boltzmann velocity distribution function ($f(v)$) as,

$$\chi_D\left(\omega_P\right) \propto \int_{-\infty}^{+\infty} \chi(\omega_p, v) f\left(v\right) dv, \tag{4}$$

where,

$$f\left(v\right) = \sqrt{\frac{m}{2\pi k_B T}}\, e^{-mv^2/2k_B T}.$$

Simulated probe transmission profiles are shown in Figures 2a and 2b. The EIA resonance is obtained due to the pump laser connecting the ground Zeeman levels $|2\rangle$, $|3\rangle$ to the excited Zeeman levels $|5\rangle$ and $|6\rangle$ whereas the Λ-EIT is induced by the control laser applied from the ground level $|1\rangle$ to the excited level $|4\rangle$. In presence of three laser beams we have obtained the EIA and EIT resonances simultaneously in a single probe profile at two separate positions of the control and the pump laser frequencies as shown in (i) and (iv) of Figures 2a and 2b. We have examined the effects of frequency tuning of the pump (Fig. 2a) and the control (Fig. 2b) lasers on the EIA and EIT resonances. For a fixed control laser frequency, if the pump laser frequency is detuned in such a way that the EIA gets merged with the EIT resonance, both of the coherent resonances being of opposite natures and equal amplitudes disappear from the probe transmission profile ((iii) of Fig. 2a). In the similar way by tuning the control laser frequency and keeping the pump laser frequency position fixed, we have again obtained the disappearance of the EIA and EIT resonances as shown in (ii) of Figure 2b. Since EIT and EIA are the coherent resonances of opposite nature, therefore when these resonances are

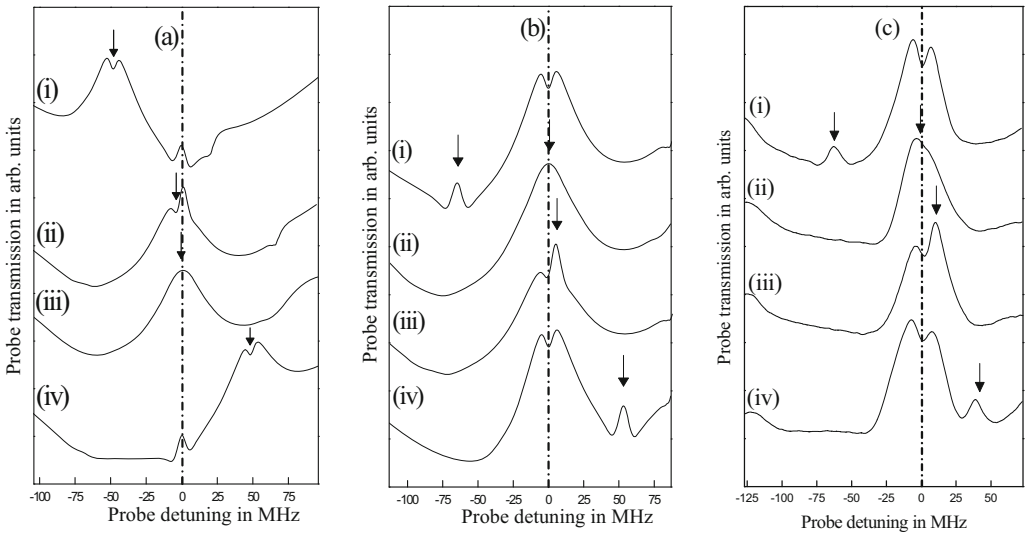

Fig. 2. Simulated probe transmission spectra against probe detuning for (a) the tuning of the pump laser from the red to blue side for a fixed frequency position of the control laser; (b) the tuning of the control laser from red to blue side for the fixed pump laser frequency position. (c) Experimentally observed probe transmission profile against probe detuning representing the shifting of the control laser frequency for a fixed pump laser frequency. Fixed frequency positions of the laser fields are indicated by the dashed dotted line and the detuned frequency positions of the laser fields are marked by the downward arrows.

tuned very close to each other then we can easily switch from absorptive to transmittive coherent resonances just by slightly detuning the pump or control laser frequencies. Theoretically we have shown that the EIA and EIT resonances can be obtained with a separation of 5 MHz ((ii) of Fig. 2a and (iii) of Fig. 2b) by tuning the pump and the control laser frequencies, respectively. In this work a simplified hypothetical model is presented to produce both the EIA and EIT resonances in a single probe Doppler profile and we have excluded rest of the hyperfine and the degenerate Zeeman levels to simplify the calculation. We have performed an experiment with three laser beams in the D_2 transition of ^{85}Rb atomic vapour to observe two opposite kinds of coherent resonances i.e. EIA and EIT simultaneously in a single probe transmission profile. The experimental energy level diagram is shown in Figure 1b. The pump laser of frequency ω_{pu} is applied from the upper ground hyperfine level $F_g = 3$ to the excited hyperfine level $F_e = 4$. The control laser of frequency ω_c is applied from lower ground hyperfine level $F_g = 2$ to the excited level $F_e = 3$. The probe laser (ω_p) is scanned from the upper ground hyperfine level $F_g = 3$ to the allowed excited levels. The control laser forms a Λ-type system with the probe laser as they connect a common excited level $F_e = 3$ to different ground hyperfine levels $F_g = 2$ and 3. This system leads to the EIT resonance at the satisfaction of the two photon resonance condition. The probe and the pump lasers induce the enhanced absorption dip i.e. EIA connecting the closed transition between two degenerate hyperfine levels $F_g = 3$ and $F_e = 4$. In the theoretical model $|1\rangle$ and $|4\rangle$ represent the ground and excited hyperfine levels $F_g = 2$ and $F_e = 3$, respectively of ^{85}Rb-D_2 transition as shown in Figure 1b. Levels $|2\rangle$, $|3\rangle$ correspond to the degenerate magnetic sublevels of the ground hyperfine level $F_g = 3$ and $|5\rangle$, $|6\rangle$ represent the degenerate magnetic sublevels corresponding to the excited hyperfine level $F_e = 4$. The amplitudes of the EIA and the EIT resonances are made almost equal in magnitude by adjusting the control and the pump laser intensities using neutral density filter (NDF). Here we have presented the experimental results corresponding to the tuning of the control laser frequency for a fixed frequency position of the pump laser near the centre of the probe Doppler profile. The observed probe transmission profiles containing both EIA and EIT resonances are shown in Figure 2c. Plots (i) and (iv) show the presence of both of the EIA and EIT resonances in a single probe Doppler profile and they disappear completely (plot (ii)) when the EIT window gets merged with the EIA resonance. Plot (iii) of Figure 2c represents the partial presence of both EIA and EIT resonances separated by ∼5 MHz. The observation of closely lying EIT and EIA resonances in the dispersive medium may be useful because it is possible to switch between the positive and negative dispersions in the same probe dispersion profile with a few MHz detuning of the pump laser.

3 Numerical simulation of observed dual-EIT resonance in N-type system

In the previous section, we have shown that using three laser fields it is possible to produce the simultaneous EIA and EIT resonances in a single probe profile. Here we have first theoretically simulated the N-type resonances in a multilevel atom due to the coherences created between the hyperfine levels in presence of three laser fields. Figure 3 represents the theoretical energy level diagram of an N-type system interacting with three lasers i.e. pump, control and probe lasers where the control laser connects

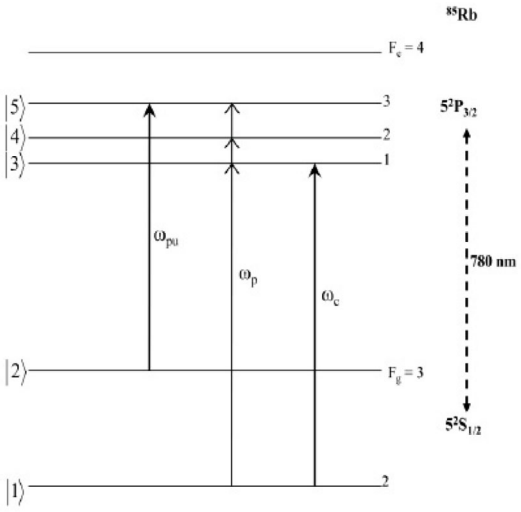

Fig. 3. Energy level diagram for an N-type system formed by the three lasers. The probe laser (ω_p) produces a V-type system with the control laser (ω_c) and a Λ-type system with the pump laser (ω_{pu}). For theoretical calculations based on this five level N-type system, the ground hyperfine levels are indicated as $|1\rangle$, $|2\rangle$ and the excited levels as $|3\rangle$, $|4\rangle$ and $|5\rangle$ on the left side.

the lower ground level $|1\rangle$ to the excited level $|3\rangle$ and the pump laser is applied from the upper ground level $|2\rangle$ to the excited level $|5\rangle$. The transition $|1\rangle \rightarrow |3\rangle$ is considered as a closed transition. The probe laser is scanned from the lower ground level $|1\rangle$ to the possible excited levels. Thus the control laser forms a V-type system whereas the pump laser constructs a Λ-type system and to study the coherent resonances in such a system we have numerically simulated the probe transmission profile. The unperturbed and the perturbation terms arising due to the atom-laser interaction are given below,

$$H_0 = \sum_{i=1}^{5} \hbar\omega_i \, |i\rangle\langle i| \tag{5}$$

$$H_p = \frac{\hbar}{2}\Big[\left(\Omega_p + \Omega_c\right)\left(|3\rangle\langle 1| + |4\rangle\langle 1| + |5\rangle\langle 1|\right) e^{-i(\omega_p+\omega_c)t} + \Omega_{pu}\left(|4\rangle\langle 2| + |5\rangle\langle 2|\right) e^{-i\omega_{pu}t} + c.c\Big]. \tag{6}$$

The Bloch equations derived from the Liouville's equation are given in detail in Appendix B. The set of equations are solved numerically under steady state condition and the Doppler-broadened probe transmission profile is obtained by including the Maxwell-Boltzmann velocity distribution function $f(v)$ as,

$$\chi_D\left(\omega_P\right) \propto \int_{-\infty}^{+\infty} \chi(\omega_p, v) f\left(v\right) dv \tag{7}$$

where,

$$\chi\left(\omega_p\right) \propto \sum_{i=3,4,5} \mathrm{Im}\left(\tilde{\rho}_{i1}\right).$$

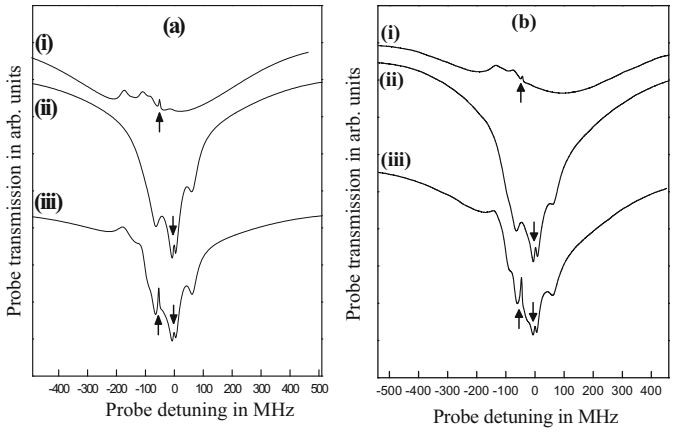

Fig. 4. (a) Numerically simulated probe transmission spectra against probe detuning for (i) V-type EIT, (ii) Λ-type EIT and (iii) dual-EIT resonance for the N-type configuration. (b) Experimentally observed (i) V-type EIT, (ii) Λ-type EIT and (iii) dual-EIT in the N-type system.

When the control laser induces the closed transition $|1\rangle \rightarrow |3\rangle$ with the probe laser connecting the transition from $|1\rangle \rightarrow |4\rangle$ forming a V-type system the coherency is created between the excited levels $|3\rangle$ and $|4\rangle$ and we obtain the V-EIT as shown by the upward arrow in (i) of Figure 4a. Apart from the V-EIT resonance, the stronger control laser burns holes in the ground state population due to the saturating effect and velocity selective resonances (VSRs) are obtained as shown in (i) of Figure 4a. Since these VSR peaks are caused by the saturation effect of the control laser these resonances are much broader than the coherent V-EIT peak. On the contrary, the pump and probe lasers form a Λ-type system connecting two different ground levels $|2\rangle$ and $|1\rangle$, respectively, to the excited level $|5\rangle$. Coherency created between the ground levels induces a Λ-EIT as shown by the downward arrow in (ii) of Figure 4a. In this configuration, the EIT resonance is obtained along with three well resolved velocity selective optical pumping (VSOP) dips and the EIT window sits on one of these VSOP dips (shown in (ii) of Fig. 4a). The VSOP dips are the signatures of enhanced probe absorption due to the pump laser induced optical pumping of atoms from the level $F_g = 3$ to $F_g = 2$ via possible excited levels. Now when the probe laser scans from $|1\rangle$ to $|5\rangle$ with the control and the pump lasers connecting the transitions $|1\rangle \rightarrow |3\rangle$ and $|2\rangle \rightarrow |5\rangle$, respectively, we obtain the dual-EIT in a single probe Doppler profile as shown in (iii) of Figure 4a. In this figure V-EIT is indicated by the upward arrow and the Λ-EIT is marked by the downward arrow. Theoretical energy level diagram of Figure 3 resembles the hyperfine structure of ^{85}Rb-D_2 transition. In the experiment, the control and the probe lasers are applied from the lower ground hyperfine level $F_g = 2$ and the pump laser is applied from the upper ground hyperfine level $F_g = 3$. The control laser connects the closed hyperfine transition $F_e = 1$ and the pump laser frequency is locked near the centre of the probe transmission profile. Figure 4b represents the experimentally obtained probe

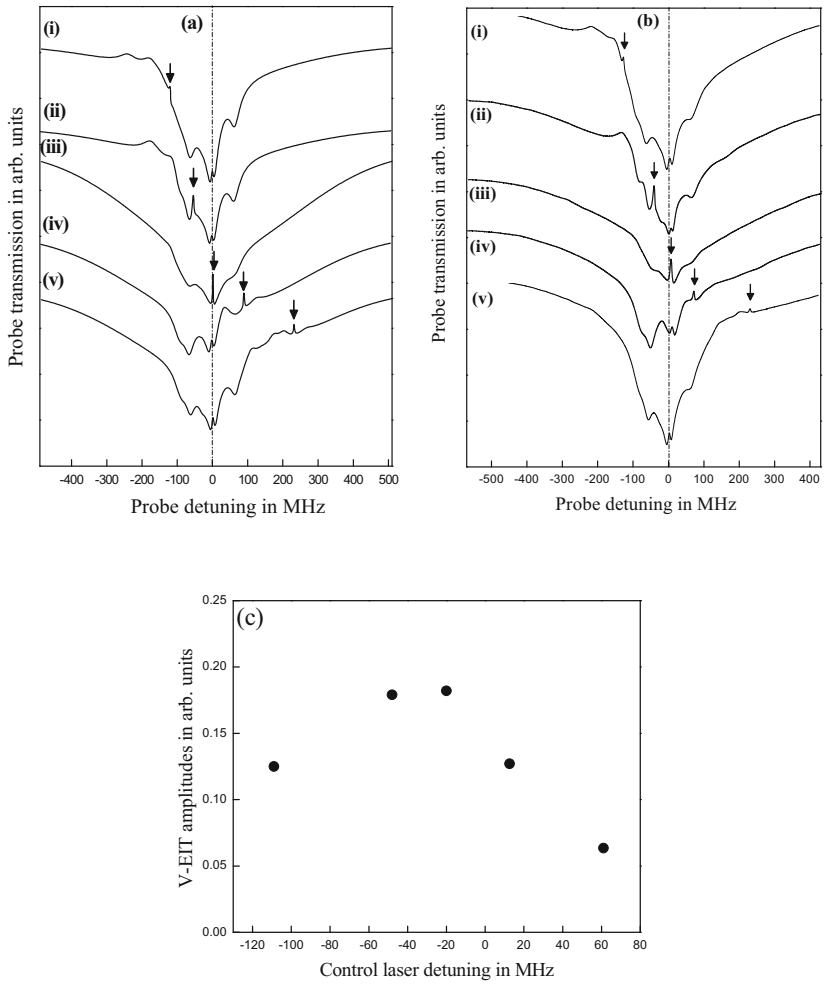

Fig. 5. (a) Plots (i)–(v) represent the simulated results for the shifting of the V-type EIT window from red to blue side over the probe Doppler profile for a fixed frequency position of the Λ-type EIT at the centre of the probe Doppler. (b) Plots (i)–(v) represent the corresponding experimental spectra of the tuning of the control laser frequency. The detuned frequency position of the control laser is marked by a downward arrow in each plot. (c) Variation of the amplitudes of the V-EIT against the detuned frequency positions of the control laser with respect to the fixed frequency position of the pump laser.

transmission profiles corresponding to the V-EIT (marked by upward arrow in plot (i)), Λ-EIT (marked by downward arrow in plot (ii)) and the dual-EIT in the N-type system (indicated by upward and downward arrows in plot (iii)) in the D_2 transition of ^{85}Rb atomic vapour. It can be seen from the theoretical, as well as the experimental results (plots (iii) of Figs. 4a and 4b) that the contrast of the V-EIT is enhanced by seven times when three lasers act together forming an N-type system. As the V-EIT falls on the VSOP dip in the Λ-type system as shown in (iii) of Figures 4a and 4b, the contrast of the V-type EIT resonance gets improved due to the availability of more number of atoms at the position of the VSOP dip.

We have also theoretically investigated the effect of frequency tuning of the control laser over the probe Doppler profile for a fixed frequency position of the pump laser and compared them with the experimental results. Theoretically simulated spectra corresponding to the tuning of the control laser frequency for a fixed frequency position of the pump laser are shown in Figure 5a. We have obtained the dual-EIT peaks in a single probe Doppler profile under the N-type configuration for any red and blue detuned frequency positions of the control laser for a fixed frequency position of the pump laser as shown in (i), (ii), (iv) and (v) of Figure 5a. The control laser frequency is detuned from $\sim$–120 MHz ((i) of Fig. 5a) to $\sim$+230 MHz ((v) of Fig. 5a) over the probe Doppler profile to shift the position of the V-EIT peak and the control detuning is zero when it is tuned to the transition $|1\rangle \rightarrow |4\rangle$. But when the V-EIT gets merged with the Λ-EIT for specific frequency position of the control laser, we get a single EIT line shape due to the superposition of the Λ and V-EIT resonances as shown in (iii) of Figure 5a. Experimentally, we have also observed the dual-EIT for the tuning of the control laser frequency over the probe Doppler profile with the fixed frequency position of the pump laser at the centre of the Doppler profile as presented in (i), (ii), (iv) and (v) of Figure 5b except when these two different types of transparency peaks get superposed with each other (plot (iii)). In both figures the fixed frequency position of the pump laser is shown by

the dotted line and the tuned positions of the control laser frequency is indicated by the downward arrow. It can be seen from Figures 5a and 5b that as the V-EIT approaches to the Λ-EIT from the far red detuned position, the EIT line shape in the V-type system gets more enhanced. As the control laser is tuned near the Λ-type EIT, it enters into the frequency range of the VSOP dips produced by the Λ-type system and the improvement in the contrast of the V-EIT is obtained. In the blue detuned position (plot (iv) of Fig. 5b), the V-EIT signal is not so much enhanced due to the less pronounced optical pumping effects. The experimentally observed variation of the amplitudes of V-EIT resonance with the detuning of the control laser is presented in Figure 5c. It shows that the amplitude of the V-EIT gradually increases when it is tuned to the position of the Λ-EIT from the far red detuned position and then again decreases when it is detuned to the blue side from the Λ-EIT position.

4 Atomic density effect on EIT in N-type system

We have also investigated the atomic density effect on the contrast of the single EIT peak obtained in the N-type configuration (Fig. 3) both theoretically and experimentally. Highly dense optical medium modifies the coherent properties of the atomic system. In our earlier work [12] we have shown experimentally and theoretically the atomic density effect on the individual Λ and V-type EIT resonances. In this present work we have theoretically simulated the density effect on the single and enhanced EIT resonance in the N-type system which is a combination of the Λ and V-type EIT systems. The optical Bloch equations for the N-type system as shown in Figure 3 are presented in Appendix B and we have solved these equations to get the N-EIT peak theoretically. Simulated Doppler broadened probe transmission profiles are shown in Figure 6a where we have presented the theoretical results corresponding to the temperatures 318 K, 328 K and 343 K. In our experiment we have increased the temperature of the vapour cell from 318 K to 343 K to observe the density effect on the single and pronounced EIT resonance obtained in the N-type system. Experimentally observed probe transmission profiles corresponding to the vapour cell temperatures varying from 318 K to 343 K are shown in Figure 6b. We can see from both theoretical and experimental observations that the amplitude of the EIT resonance in the N-type system improves for the increment in the vapour cell temperature from 318 K to 328 K and then decreases with further increase in the cell temperature. Thus the experimental observations of the density effect on the contrast of the N-EIT resonance are well agreed with the theoretical model based on the five level N-type system. The observed variation of the amplitude of the N-EIT peak with atomic vapour density is shown in Figure 7a. The N-EIT resonance is the superposition of the Λ and V-type EIT resonances. As the temperature of the cell increases from 318 K to 343 K, the

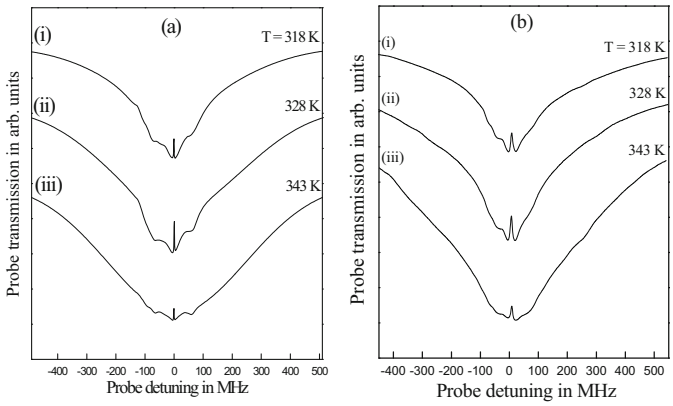

Fig. 6. Plots of (a) numerically simulated and (b) experimentally observed probe transmission spectra against probe detuning showing the variation of the single EIT resonance in the N-type system for the three different temperatures of the vapour cell (i) 318 K, (ii) 328 K and (iii) 343 K.

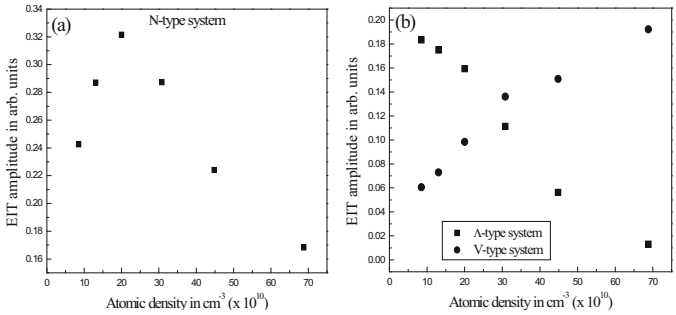

Fig. 7. Variation of the amplitude of the (a) N-EIT resonance and (b) individual Λ and V-type EIT resonances with the atomic density of the vapour cell.

atomic vapour density increases from $\sim 10^{10}$ to 10^{11} cm^{-3}. This increased atomic number density leads to the enhancement of the EIT resonance in the V-type system. But the Λ-type EIT resonance becomes smaller in amplitude with the increase in the cell temperature. In the Λ-type system the increment in the atomic number density increases the number of spontaneously emitted photons that get reabsorbed by the atoms trapped in the ground non-coupled state. The re-absorption process increases the ground state decay rates that lead to diminish the transparency peak in the Λ-type system with gradually increasing cell temperature. Since the high contrast EIT resonance in N-type system is a combined effect of the Λ and V-type EIT windows we have plotted separately the nature of variation of amplitude of the Λ and V-type EIT peaks with the vapour density as shown in Figure 7b. The amplitude of the EIT resonance in the V-type system (shown by the circles) shows an increment though for the Λ-type system it decreases (indicated by the squares). But the rate of increment of the EIT amplitude with atomic density in V-type system is not same as the decreasing rate for the Λ-type system. We have calculated the slopes of the curves shown in Figure 7b for the Λ and V-type systems separately and tabulated their ratio ($|S_{A\Lambda}|/|S_{AV}|$) in Table 1 where $S_{A\Lambda}$ and S_{AV} correspond

Table 1. Ratio of the slopes of the curves corresponding to the amplitude variation in Λ and V-type systems.

Temperature range	Atomic density in cm^{-3}	$\lvert S_{A\Lambda}\rvert/\lvert S_{AV}\rvert$
318 K–323 K	8.506×10^{10}–1.307×10^{11}	0.673
323 K–328 K	1.307×10^{11}–2×10^{11}	0.369
328 K–333 K	2×10^{11}–3.08×10^{11}	1.277
333 K–338 K	3.08×10^{11}–4.5×10^{11}	3.73

to the Λ and V-type systems, respectively. It can be commented from the ratio that the V-type system dominates over the Λ-type system for the temperature range 318 K to 328 K as $|S_{A\Lambda}|/|S_{AV}| < 1$ for that temperature region but afterwards the Λ-type system dominates because of $|S_{A\Lambda}|/|S_{AV}| > 1$. So at elevated temperatures i.e. at high atomic densities, the process of photon re-absorption by the trapped state population becomes more significant. Since the high contrast N-EIT resonance is the combined effect of Λ and V-type EIT, it shows an increment of its amplitude up to 328 K dominated by the V-type system and for the rest of the temperature range the amplitude decreases due to the more effective nature of the Λ-type system. Such kind of atomic density dependent study is important for the miniaturized cell which is operated at comparatively higher temperature.

5 Conclusion

We have presented a detail theoretical study on the quantum coherence resonances in a multilevel atomic system in presence of three laser beams. Multi coherences created between the degenerate Zeeman levels and the hyperfine levels in the atomic system produce the EIA and EIT resonances simultaneously in a single probe transmission profile. Theoretical calculation based on the density matrix formalism is performed in detail to obtain the EIA and EIT resonances in a common probe Doppler profile. We have shown that these two coherent resonances of opposite signs can be tuned very close to each other and even they completely cancel out when they are merged in the probe transmission profile. Simulated results are compared with the experimental spectra and found in good agreement for the ^{85}Rb-D_2 transition. A study of both EIA and EIT resonances in a single probe transmission profile may be of highly significant in getting fast and slow light simultaneously in a single atomic system. It will be also possible to store and retrieve light pulses in a single system due to the simultaneous presence of these two opposite types of coherent resonances in a single system. We have also theoretically calculated the dual-EIT resonance in an N-type system. Two EIT resonances are obtained when the EIT windows in the Λ and V-type systems are made separated from each other in the same probe Doppler. At the merging of these two EIT windows, we get a single EIT with improved contrast. A detail study of dual-EIT windows in a single atomic system finds promising applications in four-wave and six-wave mixing processes, storage of light pulses via two channels, etc. We have considered a hypothetical model of five levels interacting with three laser fields to theoretically produce the dual as well as the single and enhanced EIT resonance corresponding to the N-type system and the results are well agreed with the observations. Apart from the investigation of the coherent resonances in optically thin medium, it is also very useful to study the modification of the coherent resonances in highly dense optical medium for the miniaturized vapour cells. Here, we have experimentally shown the effect of atomic density on the high contrast EIT resonance in the N-type system. We have also presented the theoretical results corresponding to the density effect on the N-EIT resonance. The observations are found to agree well with the numerical results produced by the theoretical model of an N-type system.

This work is financially supported by UPE scheme of Calcutta University (UPE scheme-Holistic Dev. Research in Sc. & Tech. 2.1- Laser Group Project). Financial assistance from DST-FIST is also acknowledged. We thank Prof. P.N. Ghosh and Dr. Dimitar Slavov for their fruitful scientific discussion during our work. SD thanks UGC to provide the research fellowship under RFSMS scheme.

Appendix A

The optical Bloch equations in presence of three laser fields for the simultaneous occurrence of EIA and EIT resonances in a multilevel atomic system are explicitly expressed as follows,

$$\dot{\tilde{\rho}}_{11} = -\frac{i}{2}\Omega_c\left(\tilde{\rho}_{41} - \tilde{\rho}_{14}\right) - \Gamma_{11}^N\tilde{\rho}_{11} + \Gamma_{22}^N\tilde{\rho}_{22} + A_{41}\Gamma_4\tilde{\rho}_{44}, \tag{A.1}$$

$$\dot{\tilde{\rho}}_{22} = -\frac{i}{2}\Big[\Omega_{p42}\left(\tilde{\rho}_{42} - \tilde{\rho}_{24}\right) + \Omega_{p62}\left(\tilde{\rho}_{62} - \tilde{\rho}_{26}\right) + \Omega_{pu1}\left(\tilde{\rho}_{52} - \tilde{\rho}_{25}\right)\Big] + \Gamma_{11}^N\tilde{\rho}_{11} - 2\Gamma_{22}^N\tilde{\rho}_{22} + \Gamma_{33}^N\tilde{\rho}_{33} + A_{42}\Gamma_4\tilde{\rho}_{44} + A_{52}\Gamma_5\tilde{\rho}_{55} + A_{62}\Gamma_6\tilde{\rho}_{66}, \tag{A.2}$$

$$\dot{\tilde{\rho}}_{33} = -\frac{i}{2}\Omega_{pu2}\left(\tilde{\rho}_{63} - \tilde{\rho}_{36}\right) + \Gamma_{11}^N\tilde{\rho}_{11} + \Gamma_{22}^N\tilde{\rho}_{22} - \Gamma_{33}^N\tilde{\rho}_{33} + A_{43}\Gamma_4\tilde{\rho}_{44} + A_{63}\Gamma_6\tilde{\rho}_{66}, \tag{A.3}$$

$$\dot{\tilde{\rho}}_{44} = -\frac{i}{2}\left[\Omega_c\left(\tilde{\rho}_{14} - \tilde{\rho}_{41}\right) + \Omega_{p42}\left(\tilde{\rho}_{24} - \tilde{\rho}_{42}\right)\right] - \Gamma_4\tilde{\rho}_{44}, \tag{A.4}$$

$$\dot{\tilde{\rho}}_{55} = -\frac{i}{2}\Omega_{pu1}\left(\tilde{\rho}_{25} - \tilde{\rho}_{52}\right) - \Gamma_5\tilde{\rho}_{55}, \tag{A.5}$$

$$\dot{\tilde{\rho}}_{66} = -\frac{i}{2}\left[\Omega_{p62}\left(\tilde{\rho}_{26} - \tilde{\rho}_{62}\right) + \Omega_{pu2}\left(\tilde{\rho}_{36} - \tilde{\rho}_{63}\right)\right] - \Gamma_6\tilde{\rho}_{66}, \tag{A.6}$$

$$\dot{\tilde{\rho}}_{21} = -\left[i\left(\Delta_c - \Delta_{1p}\right) + \gamma_{21}\right]\tilde{\rho}_{21} - \frac{i}{2}\Omega_{p42}\tilde{\rho}_{41} - \frac{i}{2}\Omega_{pu1}\tilde{\rho}_{51} - \frac{i}{2}\Omega_{p62}\tilde{\rho}_{61} + \frac{i}{2}\Omega_c\tilde{\rho}_{24}, \tag{A.7}$$

$$\dot{\tilde{\rho}}_{31} = -\left[i\left(\Delta_c - \Delta_{pu2}\right) + \gamma_{31}\right]\tilde{\rho}_{31} - \frac{i}{2}\Omega_{pu2}\tilde{\rho}_{61} + \frac{i}{2}\Omega_c\tilde{\rho}_{34}, \quad (A.8)$$

$$\dot{\tilde{\rho}}_{32} = -\left[i\left(\Delta_{2p} - \Delta_{pu2}\right) + \gamma_{32}\right]\tilde{\rho}_{32} + \Gamma_6\tilde{\rho}_{65} - \frac{i}{2}\Omega_{pu2}\tilde{\rho}_{62} + \frac{i}{2}\Omega_{p42}\tilde{\rho}_{34} + \frac{i}{2}\Omega_{pu1}\tilde{\rho}_{35} + \frac{i}{2}\Omega_{p62}\tilde{\rho}_{36}, \quad (A.9)$$

$$\dot{\tilde{\rho}}_{41} = -\left(i\Delta_c + \gamma_{41}\right)\tilde{\rho}_{41} + \frac{i}{2}\Omega_c\left(\tilde{\rho}_{44} - \tilde{\rho}_{11}\right) - \frac{i}{2}\Omega_{p42}\tilde{\rho}_{21}, \quad (A.10)$$

$$\dot{\tilde{\rho}}_{42} = -\left(i\Delta_{1p} + \gamma_{42}\right)\tilde{\rho}_{42} + \frac{i}{2}\Omega_{p42}\left(\tilde{\rho}_{44} - \tilde{\rho}_{22}\right) - \frac{i}{2}\Omega_c\tilde{\rho}_{12} + \frac{i}{2}\Omega_{pu1}\tilde{\rho}_{45} + \frac{i}{2}\Omega_{p62}\tilde{\rho}_{46}, \quad (A.11)$$

$$\dot{\tilde{\rho}}_{43} = -\left(i\Delta_{1p} + \gamma_{43}\right)\tilde{\rho}_{43} - \frac{i}{2}\Omega_c\tilde{\rho}_{13} + \frac{i}{2}\Omega_{pu2}\tilde{\rho}_{46} - \frac{i}{2}\Omega_{p42}\tilde{\rho}_{23}, \quad (A.12)$$

$$\dot{\tilde{\rho}}_{51} = -\left(i\Delta_c + \gamma_{51}\right)\tilde{\rho}_{51} + \frac{i}{2}\Omega_c\tilde{\rho}_{54} - \frac{i}{2}\Omega_{pu1}\tilde{\rho}_{21}, \quad (A.13)$$

$$\dot{\tilde{\rho}}_{52} = -\left(i\Delta_{pu1} + \gamma_{52}\right)\tilde{\rho}_{52} + \frac{i}{2}\Omega_{pu1}\left(\tilde{\rho}_{55} - \tilde{\rho}_{22}\right) + \frac{i}{2}\Omega_{p42}\tilde{\rho}_{54} + \frac{i}{2}\Omega_{p62}\tilde{\rho}_{56}, \quad (A.14)$$

$$\dot{\tilde{\rho}}_{53} = -\left(i\Delta_{pu2} + \gamma_{53}\right)\tilde{\rho}_{53} + \frac{i}{2}\Omega_{pu2}\tilde{\rho}_{56} - \frac{i}{2}\Omega_{pu1}\tilde{\rho}_{23}, \quad (A.15)$$

$$\dot{\tilde{\rho}}_{54} = -\left[i\left(\Delta_{pu1} - \Delta_{1p}\right) + \gamma_{54}\right]\tilde{\rho}_{54} + \frac{i}{2}\Omega_{p42}\tilde{\rho}_{52} - \frac{i}{2}\Omega_{pu1}\tilde{\rho}_{24} + \frac{i}{2}\Omega_c\tilde{\rho}_{51}, \quad (A.16)$$

$$\dot{\tilde{\rho}}_{61} = -\left(i\Delta_c + \gamma_{61}\right)\tilde{\rho}_{61} + \frac{i}{2}\Omega_c\tilde{\rho}_{64} - \frac{i}{2}\Omega_{pu2}\tilde{\rho}_{31} - \frac{i}{2}\Omega_{p62}\tilde{\rho}_{21}, \quad (A.17)$$

$$\dot{\tilde{\rho}}_{62} = -\left(i\Delta_{2p} + \gamma_{62}\right)\tilde{\rho}_{62} + \frac{i\Omega_{p62}}{2}\left(\tilde{\rho}_{66} - \tilde{\rho}_{22}\right) + \frac{i}{2}\Omega_{pu1}\tilde{\rho}_{65} - \frac{i}{2}\Omega_{pu2}\tilde{\rho}_{32} + \frac{i}{2}\Omega_{p42}\tilde{\rho}_{64}, \quad (A.18)$$

$$\dot{\tilde{\rho}}_{63} = -\left(i\Delta_{pu2} + \gamma_{63}\right)\tilde{\rho}_{63} + \frac{i}{2}\Omega_{pu2}\left(\tilde{\rho}_{66} - \tilde{\rho}_{33}\right) - \frac{i}{2}\Omega_{p62}\tilde{\rho}_{23}, \quad (A.19)$$

$$\dot{\tilde{\rho}}_{64} = -\left[i\left(\Delta_{pu2} - \Delta_{1p}\right) + \gamma_{64}\right]\tilde{\rho}_{64} + \frac{i}{2}\Omega_{p42}\tilde{\rho}_{62} - \frac{i}{2}\Omega_{pu2}\tilde{\rho}_{34} - \frac{i}{2}\Omega_{p62}\tilde{\rho}_{24} + \frac{i}{2}\Omega_c\tilde{\rho}_{61}, \quad (A.20)$$

$$\dot{\tilde{\rho}}_{65} = -\left[i\left(\Delta_{2p} - \Delta_{pu1}\right) + \left(\gamma_{65} + \Gamma_6\right)\right]\tilde{\rho}_{65} - \frac{i}{2}\Omega_{p62}\tilde{\rho}_{25} + \frac{i}{2}\Omega_{pu1}\tilde{\rho}_{62} - \frac{i}{2}\Omega_{pu2}\tilde{\rho}_{35}. \quad (A.21)$$

Here ρ_{11}, ρ_{22}, ρ_{33}, ρ_{44}, ρ_{55}, ρ_{66} are the diagonal matrix elements that represent the corresponding level populations. Among the off-diagonal elements ρ_{42}, ρ_{62}, ρ_{63}, ρ_{52}, ρ_{41} are the coherence terms directly coupled by the probe, pump and control laser fields. Ω's are the Rabi frequencies corresponding to different laser field induced transitions. Δ's are the respective detuning terms that are defined as, $\Delta_c = (\omega_{41} - \omega_c)$, $\Delta_{pu1} = (\omega_{52} - \omega_{pu1})$, $\Delta_{pu2} = (\omega_{63} - \omega_{pu2})$ and $\Delta_{ip} = (\omega_{i2} - \omega_p)$ with $i = 4, 6$. Γ_{ii}^N $(i = 1, 2, 3)$ and γ_{j1} $(j = 2, 3)$ represent the population exchange rate between the ground levels and the coherence dephasing rate, respectively. Γ_j ($\sim 2\pi \times 6$ MHz for ^{85}Rb-D_2 transition) $(j = 4, 5, 6)$ is the spontaneous decay rate from the excited levels. In the population terms, $A_{ji}\Gamma_j\rho_{jj}$ $(i = 1, 2, 3$ and $j = 4, 5, 6)$ represents the redistribution of population among the ground hyperfine and Zeeman levels via decay from the excited levels. The second term in the equation for $\tilde{\rho}_{32}$ (Eq. (A.9)) represents the transfer of coherence from the degenerate excited Zeeman levels to the degenerate ground Zeeman levels via spontaneous emission. In our simulation we have taken $\Omega_p = 2\pi \times 4$ MHz, $\Omega_{pu} = 3\Omega_p$ and $\Omega_c = 4\Omega_p$ to obtain the EIA and EIT resonances of almost equal amplitudes. Γ_{ii}^N and γ_{j1} are set as $2\pi \times 100$ kHz and $2\pi \times 500$ kHz, respectively.

Appendix B

The optical Bloch equations for the dual-EIT resonance in multilevel atomic system interacting with three laser fields are presented in the explicit form as follows,

$$\dot{\tilde{\rho}}_{11} = \frac{i}{2}\Big[\left(\Omega_{p31} + \Omega_{c31}\right)\left(\tilde{\rho}_{13p} + \tilde{\rho}_{13c} - \tilde{\rho}_{31p} - \tilde{\rho}_{31c}\right) + \left(\Omega_{p41} + \Omega_{c41}\right)\left(\tilde{\rho}_{14p} + \tilde{\rho}_{14c} - \tilde{\rho}_{41p} - \tilde{\rho}_{41c}\right) + \left(\Omega_{p51} + \Omega_{c51}\right)\left(\tilde{\rho}_{15p} + \tilde{\rho}_{15c} - \tilde{\rho}_{51p} - \tilde{\rho}_{51c}\right)\Big] - \Gamma_1^N\tilde{\rho}_{11} + \Gamma_2^N\tilde{\rho}_{22} + A_{31}\Gamma_3\tilde{\rho}_{33} + A_{41}\Gamma_4\tilde{\rho}_{44} + A_{51}\Gamma_5\tilde{\rho}_{55}, \quad (B.1)$$

$$\dot{\tilde{\rho}}_{22} = \frac{i}{2}\Omega_{pu42}\left(\tilde{\rho}_{24} - \tilde{\rho}_{42}\right) + \frac{i}{2}\Omega_{pu52}\left(\tilde{\rho}_{25} - \tilde{\rho}_{52}\right) + \Gamma_1^N\tilde{\rho}_{11} - \Gamma_2^N\tilde{\rho}_{22} + A_{42}\Gamma_4\tilde{\rho}_{44} + A_{52}\Gamma_5\tilde{\rho}_{55}, \quad (B.2)$$

$$\dot{\tilde{\rho}}_{33} = \frac{i}{2}\left(\Omega_{p31} + \Omega_{c31}\right)\left(\tilde{\rho}_{31p} - \tilde{\rho}_{13p} + \tilde{\rho}_{31c} - \tilde{\rho}_{13c}\right) - \Gamma_3\tilde{\rho}_{33}, \quad (B.3)$$

$$\dot{\tilde{\rho}}_{44} = \frac{i}{2}\left(\Omega_{p41} + \Omega_{c41}\right)\left(\tilde{\rho}_{41p} - \tilde{\rho}_{14p} + \tilde{\rho}_{41c} - \tilde{\rho}_{14c}\right) + \frac{i}{2}\Omega_{pu42}\left(\tilde{\rho}_{42} - \tilde{\rho}_{24}\right) - \Gamma_4\tilde{\rho}_{44}, \quad (B.4)$$

$$\dot{\tilde{\rho}}_{55} = \frac{i}{2}\left(\Omega_{p51} + \Omega_{c51}\right)\left(\tilde{\rho}_{51p} - \tilde{\rho}_{15p} + \tilde{\rho}_{51c} - \tilde{\rho}_{15c}\right) + \frac{i}{2}\Omega_{pu52}\left(\tilde{\rho}_{52} - \tilde{\rho}_{25}\right) - \Gamma_5\tilde{\rho}_{55}, \quad (B.5)$$

$$\dot{\tilde{\rho}}_{21j} = -\left[i\left(\Delta_{2j} - \Delta_{1pu}\right) + \gamma_{21}\right]\tilde{\rho}_{21j} + \frac{i}{2}[\Omega_{j31}\tilde{\rho}_{23} + \Omega_{j41}\tilde{\rho}_{24} + \Omega_{j51}\tilde{\rho}_{25} - \Omega_{pu42}\tilde{\rho}_{41j} - \Omega_{pu52}\tilde{\rho}_{51j}]; [j = p, c], \quad (B.6)$$

$$\dot{\tilde{\rho}}_{31j} = -\left(i\Delta_{1j}+\gamma_{31}\right)\tilde{\rho}_{31j} + \frac{i\Omega_{j31}}{2}\left(\tilde{\rho}_{33}-\tilde{\rho}_{11}\right) + \frac{i}{2}\left(\Omega_{p41}+\Omega_{c41}\right)\tilde{\rho}_{34c} + \frac{i}{2}\left(\Omega_{p41}+\Omega_{c41}\right)\tilde{\rho}_{34pu} + \frac{i}{2}\left(\Omega_{p51}+\Omega_{c51}\right)\tilde{\rho}_{35c} + \frac{i}{2}\left(\Omega_{p51}+\Omega_{c51}\right)\tilde{\rho}_{35pu}; \left[j=p,c\right], \tag{B.7}$$

$$\dot{\tilde{\rho}}_{32} = -\left[i\Delta_{1pu}+\gamma_{32}\right]\tilde{\rho}_{32} - \frac{i}{2}\left(\Omega_{p31}+\Omega_{c31}\right)\tilde{\rho}_{12p} - \frac{i}{2}\left(\Omega_{p31}+\Omega_{c31}\right)\tilde{\rho}_{12c} + \frac{i}{2}\Omega_{pu42}\tilde{\rho}_{34c} + \frac{i}{2}\Omega_{pu42}\tilde{\rho}_{34pu} + \frac{i}{2}\Omega_{pu52}\tilde{\rho}_{35c} + \frac{i}{2}\Omega_{pu52}\tilde{\rho}_{35pu}, \tag{B.8}$$

$$\dot{\tilde{\rho}}_{41j} = -\left(i\Delta_{2j}+\gamma_{41}\right)\tilde{\rho}_{41j} + \frac{i\Omega_{j41}}{2}\left(\tilde{\rho}_{44}-\tilde{\rho}_{11}\right) - \frac{i}{2}\Omega_{pu42}\tilde{\rho}_{21j} + \frac{i}{2}\left(\Omega_{p31}+\Omega_{c31}\right)\tilde{\rho}_{43c} + \frac{i}{2}\left(\Omega_{p31}+\Omega_{c31}\right)\tilde{\rho}_{43pu} + \frac{i}{2}\left(\Omega_{p51}+\Omega_{c51}\right)\tilde{\rho}_{45c} + \frac{i}{2}\left(\Omega_{p51}+\Omega_{c51}\right)\tilde{\rho}_{45pu}; \left[j=p,c\right], \tag{B.9}$$

$$\dot{\tilde{\rho}}_{42} = -\left[i\Delta_{1pu}+\gamma_{42}\right]\tilde{\rho}_{42} - \frac{i}{2}\left(\Omega_{p41}+\Omega_{c41}\right)\tilde{\rho}_{12p} - \frac{i}{2}\left(\Omega_{p41}+\Omega_{c41}\right)\tilde{\rho}_{12c} + \frac{i}{2}\Omega_{pu42}\left(\tilde{\rho}_{44}-\tilde{\rho}_{22}\right) + \frac{i}{2}\Omega_{pu52}\tilde{\rho}_{45c} + \frac{i}{2}\Omega_{pu52}\tilde{\rho}_{45pu}, \tag{B.10}$$

$$\dot{\tilde{\rho}}_{43C} = -\left[i\left(\Delta_{2p}-\Delta_{1c}\right)+\gamma_{43}\right]\tilde{\rho}_{43c} - \frac{i}{2}\Omega_{pu42}\tilde{\rho}_{23} - \frac{i}{2}\left(\Omega_{p41}+\Omega_{c41}\right)\tilde{\rho}_{13p} - \frac{i}{2}\left(\Omega_{p41}+\Omega_{c41}\right)\tilde{\rho}_{13c} + \frac{i}{2}\left(\Omega_{p31}+\Omega_{c31}\right)\tilde{\rho}_{41p} + \frac{i}{2}\left(\Omega_{p31}+\Omega_{c31}\right)\tilde{\rho}_{41c}, \tag{B.11}$$

$$\dot{\tilde{\rho}}_{43pu} = -\left[i\left(\Delta_{2p}-\Delta_{1p}\right)+\gamma_{43}\right]\tilde{\rho}_{43pu} - \frac{i}{2}\Omega_{pu42}\tilde{\rho}_{23} - \frac{i}{2}\left(\Omega_{p41}+\Omega_{c41}\right)\tilde{\rho}_{13p} - \frac{i}{2}\left(\Omega_{p41}+\Omega_{c41}\right)\tilde{\rho}_{13c} + \frac{i}{2}\left(\Omega_{p31}+\Omega_{c31}\right)\tilde{\rho}_{41p} + \frac{i}{2}\left(\Omega_{p31}+\Omega_{c31}\right)\tilde{\rho}_{41c}, \tag{B.12}$$

$$\dot{\tilde{\rho}}_{51j} = -\left(i\Delta_{3j}+\gamma_{51}\right)\tilde{\rho}_{51j} + \frac{i\Omega_{j51}}{2}\left(\tilde{\rho}_{55}-\tilde{\rho}_{11}\right) - \frac{i}{2}\Omega_{pu52}\tilde{\rho}_{21j} + \frac{i}{2}\left(\Omega_{p31}+\Omega_{c31}\right)\tilde{\rho}_{53c} + \frac{i}{2}\left(\Omega_{p31}+\Omega_{c31}\right)\tilde{\rho}_{53pu} + \frac{i}{2}\left(\Omega_{p41}+\Omega_{c41}\right)\tilde{\rho}_{54c} + \frac{i}{2}\left(\Omega_{p41}+\Omega_{c41}\right)\tilde{\rho}_{54pu}; \left[j=p,c\right], \tag{B.13}$$

$$\dot{\tilde{\rho}}_{52} = -\left[i\Delta_{2pu}+\gamma_{52}\right]\tilde{\rho}_{52} - \frac{i}{2}\left(\Omega_{p51}+\Omega_{c51}\right)\tilde{\rho}_{12p} - \frac{i}{2}\left(\Omega_{p51}+\Omega_{c51}\right)\tilde{\rho}_{12c} + \frac{i}{2}\Omega_{pu52}\left(\tilde{\rho}_{55}-\tilde{\rho}_{22}\right) + \frac{i}{2}\Omega_{pu42}\tilde{\rho}_{54c} + \frac{i}{2}\Omega_{pu42}\tilde{\rho}_{54pu}, \tag{B.14}$$

$$\dot{\tilde{\rho}}_{53C} = -\left[i\left(\Delta_{3p}-\Delta_{1c}\right)+\gamma_{53}\right]\tilde{\rho}_{53c} - \frac{i}{2}\Omega_{pu52}\tilde{\rho}_{23} - \frac{i}{2}\left(\Omega_{p51}+\Omega_{c51}\right)\tilde{\rho}_{13p} - \frac{i}{2}\left(\Omega_{p51}+\Omega_{c51}\right)\tilde{\rho}_{13c} - \frac{i}{2}\left(\Omega_{p31}+\Omega_{c31}\right)\tilde{\rho}_{51p} - \frac{i}{2}\left(\Omega_{p31}+\Omega_{c31}\right)\tilde{\rho}_{51c}, \tag{B.15}$$

$$\dot{\tilde{\rho}}_{53pu} = -\left[i\left(\Delta_{3p}-\Delta_{1p}\right)+\gamma_{53}\right]\tilde{\rho}_{53pu} - \frac{i}{2}\Omega_{pu52}\tilde{\rho}_{23} - \frac{i}{2}\left(\Omega_{p51}+\Omega_{c51}\right)\tilde{\rho}_{13p} - \frac{i}{2}\left(\Omega_{p51}+\Omega_{c51}\right)\tilde{\rho}_{13c} - \frac{i}{2}\left(\Omega_{p31}+\Omega_{c31}\right)\tilde{\rho}_{51p} - \frac{i}{2}\left(\Omega_{p31}+\Omega_{c31}\right)\tilde{\rho}_{51c}, \tag{B.16}$$

$$\dot{\tilde{\rho}}_{54k} = -\left[i\left(\Delta_{3p}-\Delta_{2p}\right)+\gamma_{54}\right]\tilde{\rho}_{54k} - \frac{i}{2}\Omega_{pu52}\tilde{\rho}_{24} - \frac{i}{2}\Omega_{pu42}\tilde{\rho}_{52} - \frac{i}{2}\left(\Omega_{p51}+\Omega_{c51}\right)\tilde{\rho}_{14p} - \frac{i}{2}\left(\Omega_{p51}+\Omega_{c51}\right)\tilde{\rho}_{14c} - \frac{i}{2}\left(\Omega_{p41}+\Omega_{c41}\right)\tilde{\rho}_{51p} - \frac{i}{2}\left(\Omega_{p41}+\Omega_{c41}\right)\tilde{\rho}_{51c}; \left[k=c,pu\right]. \tag{B.17}$$

In this set of equations, ρ_{ii} ('i' runs from 1 to 5) are the level population term; ρ_{31j}, ρ_{41j}, ρ_{51j} are the coherence terms directly coupled by the probe ($j \equiv p$) and control ($j \equiv c$) lasers and ρ_{42}, ρ_{52} are the terms coupled by the pump laser. Here, $\Delta_c = (\omega_{i1} - \omega_c)$ with $i = 3, 4, 5$; $\Delta_{pu} = (\omega_{j2} - \omega_{pu})$ ($j = 4, 5$) and $\Delta_{ip} = (\omega_{i1} - \omega_p)$ with $i = 3, 4, 5$. In the dual-EIT system γ_{21} and γ_{43} are the coherence dephasing rates for the Λ and V-type EIT systems, respectively and Γ_{ii}^{N} ($i = 1, 2$) is the population exchange rate between the ground hyperfine levels. To obtain the EIT windows we have taken $\Omega_p = 2\pi \times 5$ MHz, $\Omega_{pu} = 3.5\Omega_p$ and $\Omega_c = 2.5\Omega_p$. γ_{21} and γ_{43} are set at $2\pi\times2.5$ and $2\pi\times4.5$ MHz, respectively, and Γ_{ii}^{N} is taken as $2\pi \times 100$ kHz. Here we have simulated the dual-EIT forming an N-type system considering the hyperfine levels only. Hence in this case, $A_{ji}\Gamma_j\rho_{jj}$ ($i = 1, 2$ and $j = 3, 4, 5$) represents the population redistribution among the ground levels due to the hyperfine optical pumping of atoms induced by pump and the control laser fields.

References

1. E. Arimondo, Prog. Opt. **35**, 257 (1996)
2. S.E. Harris, Phys. Today **50**, 36 (1997)
3. K.J. Boller, A. Imamoglu, S.E. Harris, Phys. Rev. Lett. **66**, 2593 (1991)
4. A.V. Taichenachev, A.M. Tumaikin, V.I. Yudin, Phys. Rev. A **61**, 011802(R) (1999)
5. A. Lezama, S. Barreiro, A.M. Akulshin, Phys. Rev. A **59**, 4732 (1999)
6. M.D. Lukin, Rev. Mod. Phys. **75**, 457 (2003)
7. A. Dogariu, A. Kuzmich, H. Cao, L.J. Wang, Opt. Express **8**, 344 (2001)

8. D.J. Fulton, S. Shepherd, R.R. Moseley, B.D. Sinclair, M.H. Dunn, Phys. Rev. A **52**, 2302 (1995)
9. G.R. Welch, G.G. Padmabandu, E.S. Fry, M.D. Lukin, D.E. Nikonov, F. Sander, M.O. Scully, A. Weis, F.K. Tittel, Found. Phys. **28**, 621 (1998)
10. M. Xiao, Y.Q. Li, S.Z. Jin, J. Gea-Banacloche, Phys. Rev. Lett. **74**, 666 (1995)
11. S. Mitra, M.M. Hossain, B. Ray, P.N. Ghosh, S. Cartaleva, D. Slavov, Opt. Commun. **283**, 1500 (2010)
12. S. Mitra, S. Dey, M.M. Hossain, P.N. Ghosh, B. Ray, J. Phys. B **46**, 075002 (2013)
13. B.P. Hou, S.J. Wang, W.L. Yu, W.L. Sun, Phys. Rev. A **69**, 053805 (2004)
14. B.P. Hou, S.J. Wang, W.L. Yu, W.L. Sun, J. Phys. B **38**, 1419 (2005)
15. Y. Gu, L. Wang, K. Wang, C. Yang, Q. Gong, J. Phys. B **39**, 463 (2006)
16. L.B. Kong, X.H. Tu, J. Wang, Y. Zhu, M.S. Zhan, Opt. Commun. **269**, 362 (2007)
17. M.M. Hossain, S. Mitra, P. Poddar, C. Chaudhuri, B. Ray, P.N. Ghosh, J. Phys. B **44**, 115501 (2011) and references therein
18. Y. Zhang, A.W. Brown, M. Xiao, Phys. Rev. Lett. **99**, 123603 (2007)
19. Y. Chen, X.G. Wei, B.S. Ham, J. Phys. B **42**, 065506 (2009)
20. M.A. Antón, F. Carreño, O.G. Calderón, S. Melle, I. Gonzalo, Opt. Commun. **281**, 6040 (2008)
21. J. Sheng, X. Yang, U. Khadka, M. Xiao, Opt. Express **19**, 17059 (2011)
22. S.D. Badger, I.G. Hughes, C.S. Adams, J. Phys. B **34**, L749 (2001)
23. M. Kwon, K. Kim, H.S. Moon, H.D. Park, J.B. Kim, J. Phys. B **34**, 2951 (2001)
24. S. Briaudeau, D. Bloch, M. Ducloy, Europhys. Lett. **35**, 337 (1996)
25. D.A. Smith, I.G. Hughes, Am. J. Phys. **72**, 631 (2004)
26. L.P. Maguire, R.M.W. van Bijnen, E. Mese, R.E. Scholten, J. Phys. B **39**, 2709 (2006)
27. M.L. Harris, C.S. Adams, S.L. Cornish, I.C. McLeod, E. Tarleton, I.G. Hughes, Phys. Rev. A **73**, 062509 (2006)
28. H.D. Do, G. Moon, H.R. Noh, Phys. Rev. A **77**, 032513 (2008)
29. H.D. Do, M.S. Heo, G. Moon, H.R. Noh, W. Jhe, Opt. Commun. **281**, 4042 (2008)
30. J. Sagle, R.K. Namiotka, J. Huennekens, J. Phys. B **29**, 2629 (1996)